

**Syntheses and properties of pH-directed two types of cobalt-lanthanoid heterometallic complexes
constructed from 2,5-dichlorobenzoate and 1,10-phenanthroline**

Yue Shen^{a,b}, Jiu-Zeng Jin^b, Zhen-Yu Yang^a, Jie Zhao^a, Bin-Qiu Liu^{a,*}, Ju-Wen Zhang^{a,*}

^aDepartment of Chemistry, Bohai University, Jinzhou 121013, P.R. China

^bDepartment of Chemistry, College of Science, Northeastern University, Shenyang 110819, P.R. China

Table S1

The SHAPE 2.1 analysis of the Sm1 ion in **2**.

code	lable	shape	symmtry	distortion (τ)
1	OP-8	Octagon	D8h	31.721
2	HPY-8	Heptagonal pyramid	C7v	22.889
3	HBPY-8	Hexagonal bipyramid	D6h	16.750
4	CU-8	Cube	Oh	10.893
5	SAPR-8	Square antiprism	D4d	1.922
6	TDD-8	Triangular dodecahedron	D2d	1.575
7	JGBF-8	Johnson gyrobifastigium J26	D2d	14.185
8	JETBPY-8	Johnson elongated triangular bipyramid J14	D3h	28.150
9	JBTPR-8	Biaugmented trigonal prism J50	C2v	2.715
10	BTPR-8	Biaugmented trigonal prism	C2v	2.009
11	JSD-8	Snub diphenoïd J84	D2d	3.848
12	TT-8	Triakis tetrahedron	Td	11.498
13	ETBPY-8	Elongated trigonal bipyramid	D3h	23.568

Table S2

The SHAPE 2.1 analysis of the Co1 ion in **2**.

code	lable	shape	symmtry	distortion (τ)
1	PP-5	Pentagon	D5h	29.383
2	vOC-5	Vacant octahedron	C4v	2.630
3	TBPY-5	Trigonal bipyramid	D3h	2.412
4	SPY-5	Spherical square pyramid	C4v	3.159
5	JTBPY-5	Johnson trigonal bipyramid J12	D3h	4.444

Table S3

Selected bond lengths (Å) for **1–8**.

	1	2	3	4			
Nd1–O1	2.396(2)	Sm1–O2	2.341(2)	Eu1–O1	2.382(2)	Gd1–O1	2.351(2)
Nd1–O3	2.341(3)	Sm1–O3	2.472(2)	Eu1–O3	2.329(3)	Gd1–O2	2.344(2)
Nd1–O4	2.368(2)	Sm1–O6	2.371(2)	Eu1–O4	2.356(2)	Gd1–O3	2.321(2)
Nd1–O7	2.361(3)	Sm1–O7	2.346(2)	Eu1–O5	2.328(3)	Gd1–O4	2.376(2)
Nd1–O10	2.337(3)	Sm1–O9	2.362(2)	Eu1–O7	2.350(2)	Gd1–O7	2.319(2)
Nd1–O1#1	2.623(3)	Sm1–O11	2.399(2)	Eu1–O1#1	2.615(3)	Gd1–O4#1	2.608(2)
Nd1–O5#1	2.470(3)	Sm1–O5#1	2.380(2)	Eu1–O2#1	2.454(3)	Gd1–O6#1	2.359(2)
Nd1–O6#1	2.376(3)	Sm1–O11#1	2.623(2)	Eu1–O6#1	2.369(2)	Gd1–O10#1	2.445(2)
Co1–O2	2.022(3)	Co1–O1	2.019(3)	Co1–O8	2.018(3)	Co1–O5	2.025(3)

* Corresponding authors.

E-mail addresses: liubinqui@126.com (B.-Q. Liu), zhangjw@bhu.edu.cn (J.-W. Zhang).

Co1–O8	2.016(3)	Co1–O8	2.022(3)	Co1–O9	2.018(3)	Co1–O8	2.019(3)
Co1–O9	2.023(3)	Co1–O10	2.024(3)	Co1–O10	2.014(3)	Co1–O9	2.023(3)
Co1–N1	2.070(3)	Co1–N1	2.076(3)	Co1–N1	2.073(3)	Co1–N1	2.077(3)
Co1–N2	2.147(4)	Co1–N2	2.152(3)	Co1–N2	2.153(4)	Co1–N2	2.153(3)
5		6		7		8	
Tb1–O1	2.355(3)	Dy1–O1	2.347(2)	Er1–O1	2.327(2)	Yb1–O4	2.273(3)
Tb1–O2	2.293(3)	Dy1–O3	2.316(2)	Er1–O2	2.297(3)	Yb1–O5	2.242(3)
Tb1–O4	2.328(3)	Dy1–O4	2.325(2)	Er1–O4	2.302(3)	Yb1–O7	2.266(3)
Tb1–O7	2.320(3)	Dy1–O5	2.291(2)	Er1–O5	2.272(3)	Yb1–O8	2.244(3)
Tb1–O10	2.297(3)	Dy1–O7	2.292(2)	Er1–O8	2.262(3)	Yb1–O10	2.300(3)
Tb1–O1#1	2.587(3)	Dy1–O1#1	2.590(2)	Er1–O1#1	2.570(3)	Yb1–O1#1	2.280(3)
Tb1–O5#1	2.417(3)	Dy1–O2#1	2.411(2)	Er1–O3#1	2.384(3)	Yb1–O3#1	2.358(3)
Tb1–O8#1	2.340(3)	Dy1–O6#1	2.331(2)	Er1–O6#1	2.311(3)	Yb1–O10#1	2.563(3)
Co1–O3	2.016(3)	Co1–O8	2.020(3)	Co1–O7	2.016(3)	Co1–O2	2.012(3)
Co1–O6	2.013(3)	Co1–O9	2.016(3)	Co1–O9	2.015(3)	Co1–O6	2.011(4)
Co1–O9	2.007(4)	Co1–O10	2.018(3)	Co1–O10	2.014(3)	Co1–O9	2.010(4)
Co1–N1	2.145(4)	Co1–N1	2.077(3)	Co1–N1	2.076(3)	Co1–N1	2.070(4)
Co1–N2	2.070(3)	Co1–N2	2.153(3)	Co1–N2	2.151(4)	Co1–N2	2.141(5)

Symmetry codes: for **1**: #1 1 –x, 1 –y, 1 –z. For **2**: #1 –x, –y, 1 –z. For **3**: #1 1 –x, 1 –y, 1 –z. For **4**: #1 1 –x, 1 –y, 1 –z. For **5**: #1 1 –x, 1 –y, 1 –z. For **6**: #1 1 –x, 1 –y, 1 –z. For **7**: #1 1 –x, 1 –y, 1 –z. For **8**: #1 1 –x, 1 –y, 1 –z.

Table S4

The SHAPE 2.1 analysis of the Sm1 ion in **2a**.

code	lable	shape	symmtry	distortion (τ)
1	OP-8	Octagon	D8h	29.377
2	HPY-8	Heptagonal pyramid	C7v	21.910
3	HBPY-8	Hexagonal bipyramid	D6h	17.074
4	CU-8	Cube	Oh	10.831
5	SAPR-8	Square antiprism	D4d	1.118
6	TDD-8	Triangular dodecahedron	D2d	3.084
7	JGBF-8	Johnson gyrobifastigium J26	D2d	16.700
8	JETBPY-8	Johnson elongated triangular bipyramid J14	D3h	25.707
9	JBTPR-8	Biaugmented trigonal prism J50	C2v	3.395
10	BTPR-8	Biaugmented trigonal prism	C2v	2.402
11	JSD-8	Snub diphenoïd J84	D2d	5.982
12	TT-8	Triakis tetrahedron	Td	11.618
13	ETBPY-8	Elongated trigonal bipyramid	D3h	21.430

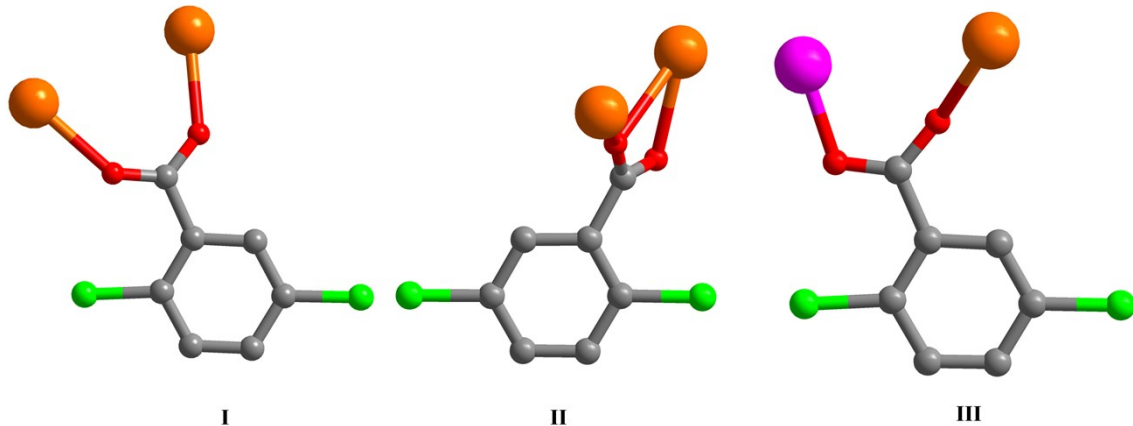
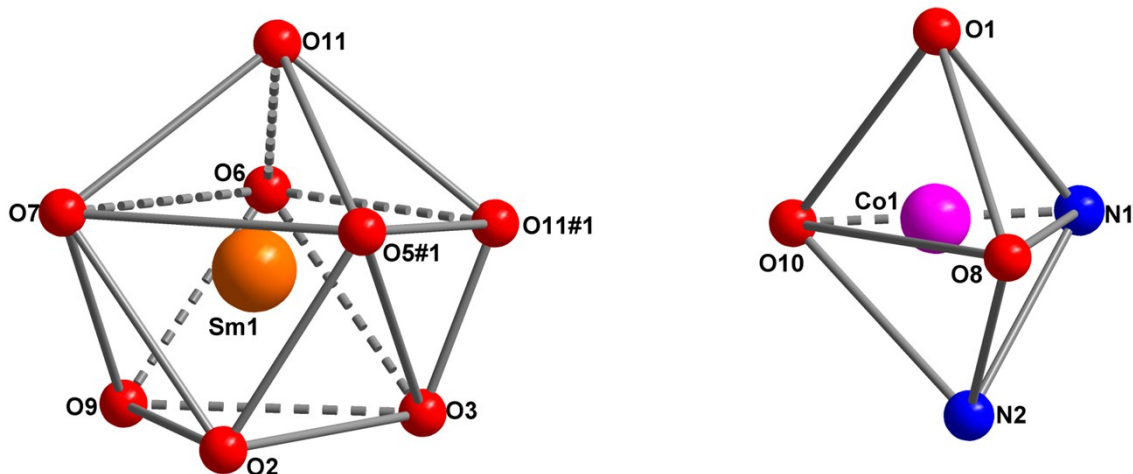
Table S5

The SHAPE 2.1 analysis of the Co1 ion in **2a**.

code	lable	shape	symmtry	distortion (τ)
1	PP-5	Pentagon	D5h	34.158
2	vOC-5	Vacant octahedron	C4v	4.864
3	TBPY-5	Trigonal bipyramid	D3h	0.734
4	SPY-5	Spherical square pyramid	C4v	2.771

Table S6Selected bond lengths (\AA) for **1a–3a**.

	1a	2a	3a
Nd1–O1	2.569(3)	Sm1–O1	2.441(2)
Nd1–O2	2.475(3)	Sm1–O2	2.452(2)
Nd1–O3	2.465(3)	Sm1–O3	2.371(2)
Nd1–O4	2.410(3)	Sm1–O5	2.536(2)
Nd1–O8	2.453(3)	Sm1–O7	2.385(2)
Nd1–O10	2.476(3)	Sm1–O9	2.425(2)
Nd1–O6#1	2.433(3)	Sm1–O6#1	2.436(2)
Nd1–O10#1	2.476(3)	Sm1–O8#1	2.406(2)
Co1–O1	2.025(3)	Co1–O4	2.011(2)
Co1–O5	2.012(3)	Co1–O5	2.034(2)
Co1–O7	1.986(4)	Co1–O10	2.034(2)
Co1–N1	2.068(3)	Co1–N1	2.070(3)
Co1–N2	2.138(4)	Co1–N2	2.070(3)

Symmetry codes: for **1a**: #1 $1 - x, 1 - y, 1 - z$. For **2a**: #1 $1 - x, 1 - y, 1 - z$. For **3a**: #1 $1 - x, 1 - y, 1 - z$.**Fig. S1.** Three types of coordination modes of the 2,5-DCB anion in **2**.**Fig. S2.** Coordination geometries of the metal ions in **2**.

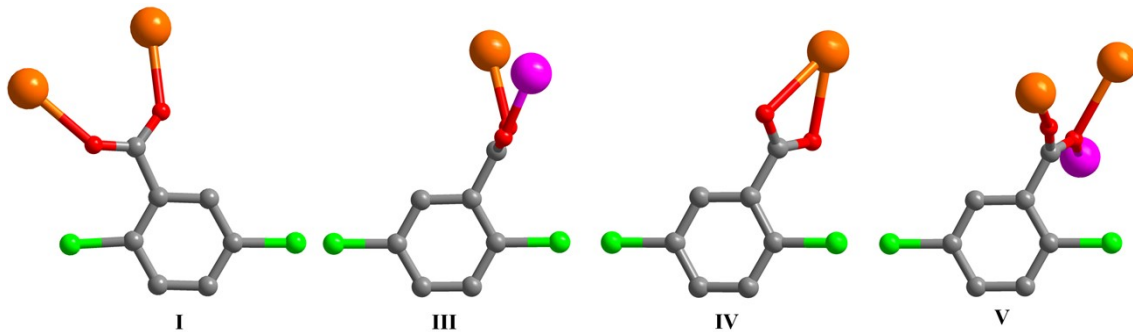


Fig. S3. Four types of coordination modes of the 2,5-DCB anion in **2a**.

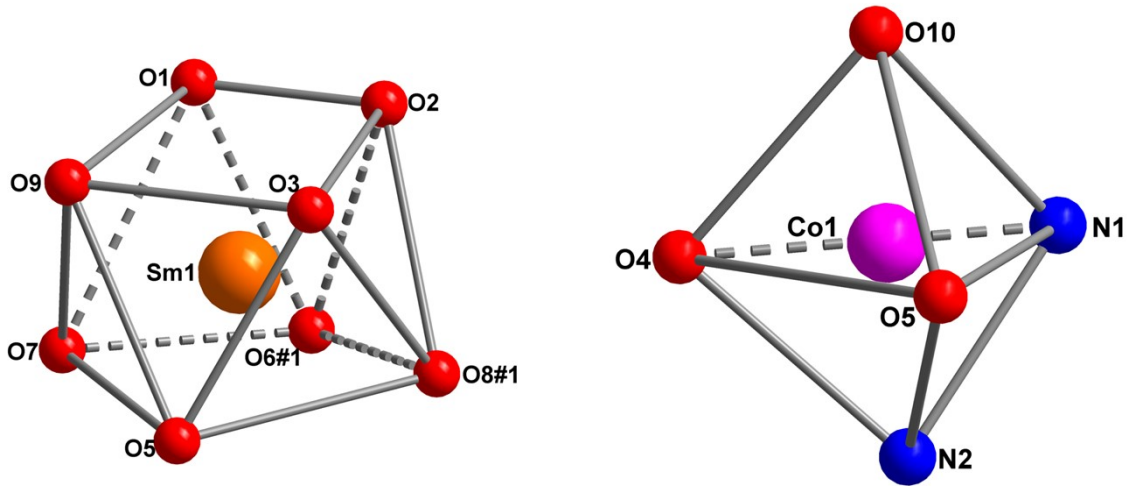


Fig. S4. Coordination geometries of the metal ions in **2a**.

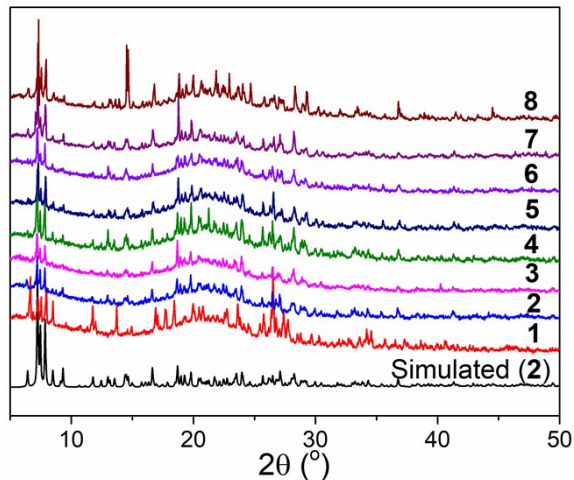


Fig. S5. Simulated PXRD pattern of **2** and as-synthesized PXRD patterns of **1–8**.

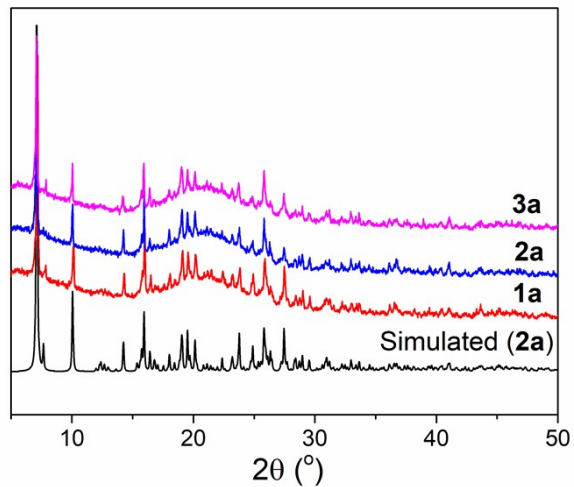


Fig. S6. Simulated PXRD pattern of **2a** and as-synthesized PXRD patterns of **1a–3a**.

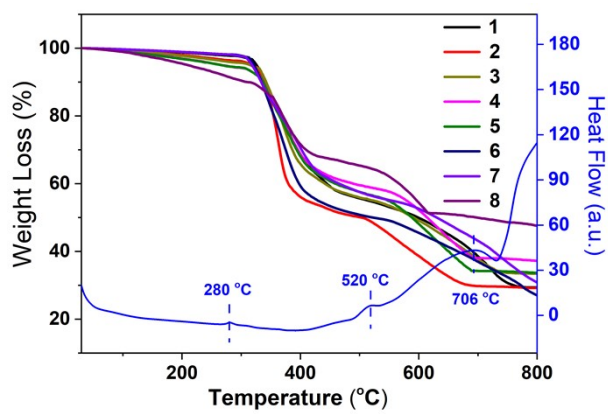


Fig. S7. TG curves of **1–8** and DTA curve of **2**.

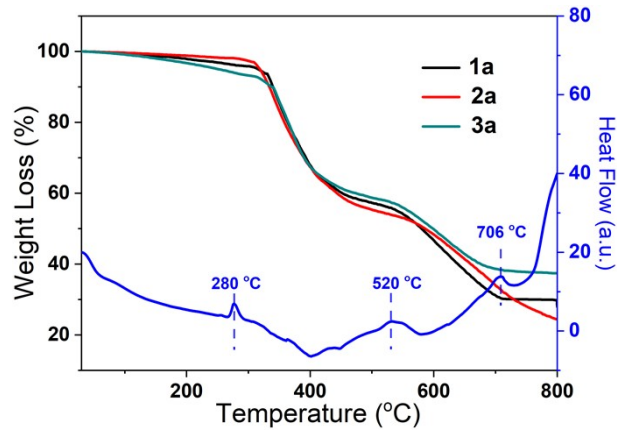


Fig. S8. TG curves of **1a–3a** and DTA curve of **2a**.

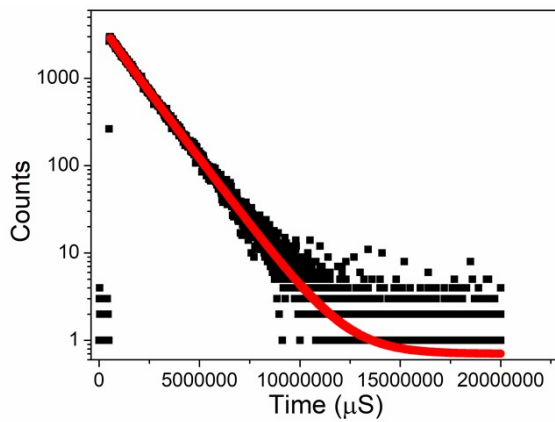


Fig. S9. Emission decay of **3** measured with $\lambda_{\text{ex}} = 351$ nm and $\lambda_{\text{em}} = 614$ nm. Solid line is a fit to the bi-exponential function.

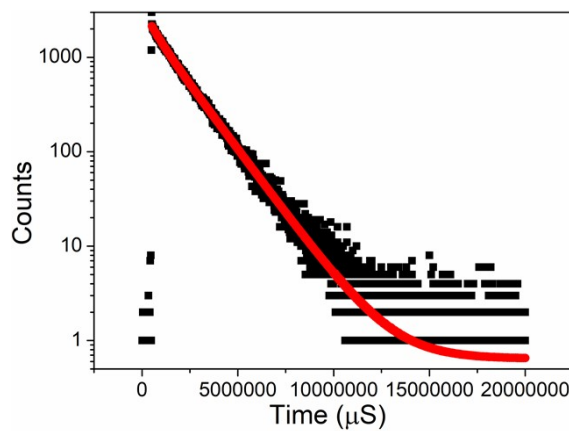


Fig. S10. Emission decay of **3a** measured with $\lambda_{\text{ex}} = 304$ nm and $\lambda_{\text{em}} = 615$ nm. Solid line is a fit to the bi-exponential function.

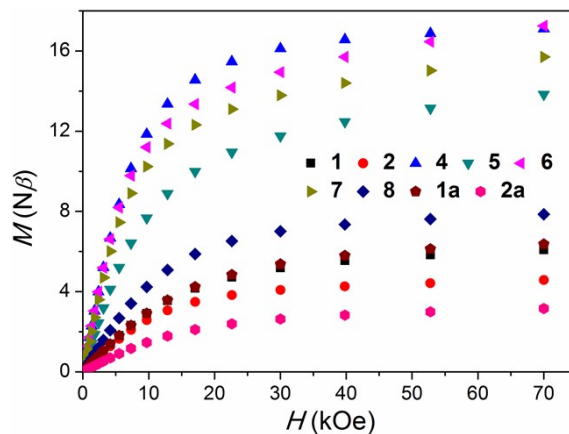


Fig. S11. M versus H plots for **1**, **2**, **1a**, **2a**, and **4–8** at 2 K.

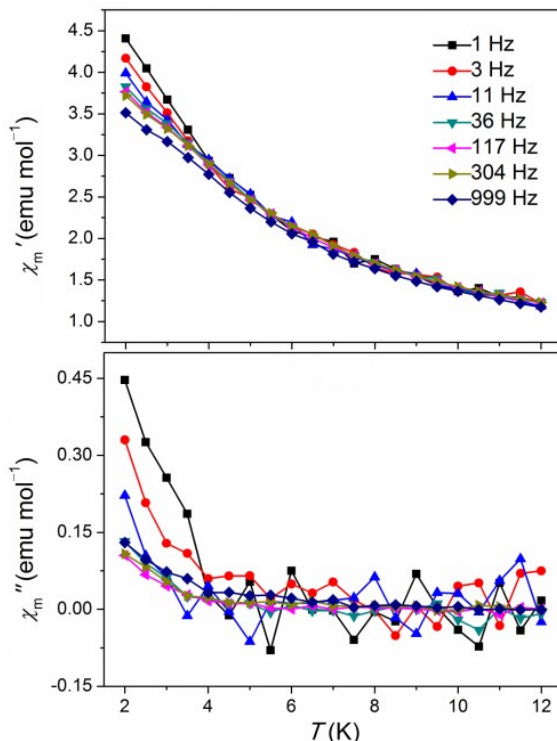


Fig. S12. Temperature dependence of the in-phase (χ') (top) and out-of-phase (χ'') (bottom) AC magnetic susceptibilities for **6** under 2000 Oe DC field at different frequencies.

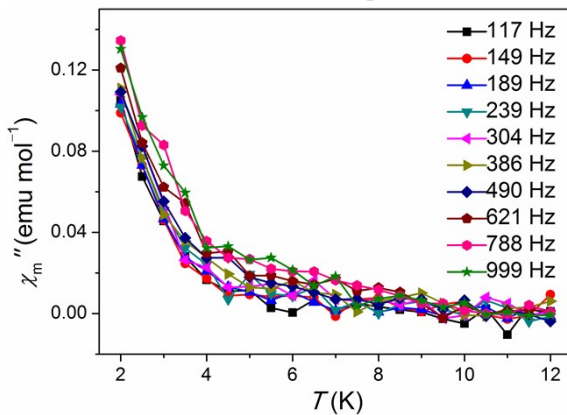


Fig. S13. Temperature dependence of the out-of-phase (χ'') AC magnetic susceptibilities for **6** under 2000 Oe DC field above 100 Hz.

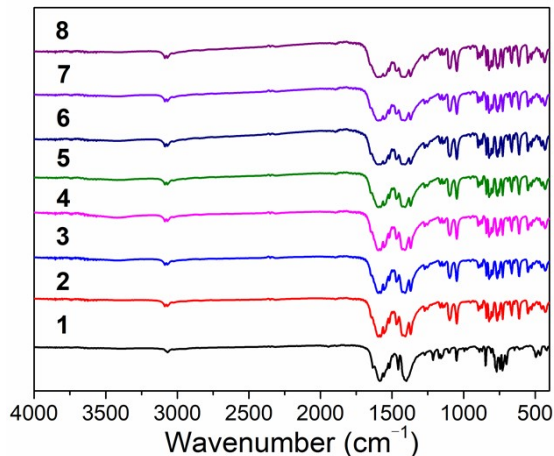


Fig. S14. FT-IR spectra of 1–8.

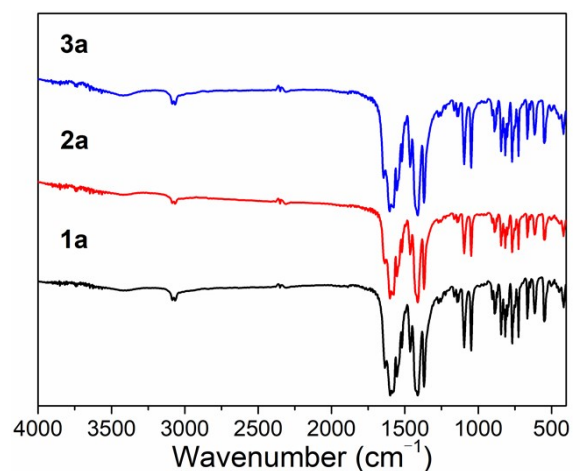


Fig. S15. FT-IR spectra of 1a–3a.